Check for updates

Distinct spatiotemporal patterns of syntactic and semantic processing in human inferior frontal gyrus

Yanming Zhu [1,2,3,9], Min Xu [4,5,9], Junfeng Lu [1,2,9], Jianhua Hu [6,9], Veronica P. Y. Kwok[5], Yulong Zhou [5], Di Yuan[5], Bin Wu[1,2], Jie Zhang[1,2], Jinsong Wu [1,2,7,8 ✉] and Li Hai Tan [3,5 ✉]

Human languages are based on syntax, a set of rules which allow an infinite number of meaningful sentences to be constructed from a finite set of words. A theory associated with Chomsky and others holds that syntax is a mind-internal, universal structure independent of semantics. This theory, however, has been challenged by studies of the Chinese language showing that syntax is processed under the semantic umbrella, and is secondary and not independent. Here, using intracranial high-density electrocorticography, we find distinct spatiotemporal patterns of neural activity in the left inferior frontal gyrus that are specifically associated with syntactic and semantic processing of Chinese sentences. These results suggest that syntactic processing may occur before semantic processing. Our findings are consistent with the view that the human brain implements syntactic structures in a manner that is independent of semantics.

Human language is a unique communication system for its complexity of syntactic structure that enables us to convey infinite ideas from finite words in novel ways. One prominent linguistic theory proposed by Noam Chomsky and many others assumes that the syntactic computational system is a core component of human language, which generates internal representations and maps them into the sensory–motor (phonological) and conceptual–intentional (semantic) systems[1,2]. This theory has led to a longstanding tradition of distinguishing specialized modular centres for syntactic processing from other linguistic components in the brain[3–9]. Supportive evidence for the modularity of syntax has come from lesion studies, which demonstrate that agrammatic aphasia can occur in people with focal brain lesions (particularly in the Broca's area and nearby structures)[10–12], and many neuroimaging studies that identify brain regions specifically involved in syntactic processing in the left inferior frontal gyrus (IFG)[5,6,13–17]. Moreover, neurophysiological studies have demonstrated that the syntactic subcomponent constitutes a module of language that is processed before semantic information[18–20].

In contrast to the modularity view, there is growing evidence showing that both syntactic and semantic processing activates a frontal–temporal network including IFG and middle/superior temporal areas, but none of these areas is strictly syntax or semantic specific[21–27], leading to a different position that the processing of syntactic and semantic information is highly integrated, rather than according to regionally dedicated modules[28–30]. In line with the neuroimaging evidence, aphasia research also reveals that patients with syntactic deficits do not have a common lesion in the brain[28,31,32].

The findings in favour of either independent or non-independent processing of syntax and semantics each seem to pose a challenge to the other. However, the two theoretical positions are not necessarily mutually exclusive. It could be the case that the human brain instantiates the modularity of syntax at a finer scale, such that syntactic and semantic processes may be implemented by different subnetworks of cells distributed within the critical language region such as IFG. Yet the dissociations at the finer spatiotemporal scale cannot be reliably differentiated with traditional functional imaging techniques.

To test this possibility, we used high-density electrocorticography (ECoG) and examined whether syntactic and semantic processes could be dissociated in the left IFG at a fine-grained level of functional organization. While previous studies are mainly conducted with functional magnetic resonance imaging (fMRI) or event-related potential (ERP), which are limited in revealing finer-grained levels of functional organization underlying language processing, high-density ECoG provides millimetre resolution in space, and millisecond resolution in time, which allows us to establish precise functional anatomical correlates and timing of neurophysiological mechanisms at the circuit level[33]. Moreover, we tested the hypothesis in Chinese, a non-inflected language that lacks morphological devices and largely relies on contextual semantics[34]. It has virtually no conjugation for verbs and no declension for nouns[35]. ERP studies showed that syntactic processing was not necessary for the initiation of semantic integration in Chinese, and failure to conduct syntactic category analysis did not block semantic access[36–39], although there was evidence showing that the syntactic processes appear earlier than the semantic processes during Chinese sentence

[1]Neurologic Surgery Department, Huashan Hospital, Shanghai Medical College, Fudan University, Shanghai, China. [2]Brain Function Laboratory, Neurosurgical Institute of Fudan University, Shanghai, China. [3]Guangdong-Hongkong-Macau Institute of CNS Regeneration and Ministry of Education CNS Regeneration Collaborative Joint Laboratory, Jinan University (Shenzhen), Shenzhen, China. [4]Center for Brain Disorders and Cognitive Sciences, School of Psychology, Shenzhen University, Shenzhen, China. [5]Center for Language and Brain, Shenzhen Institute of Neuroscience, Shenzhen, China. [6]Institute of Linguistics, Chinese Academy of Social Sciences, Beijing, China. [7]Institute of Brain-Intelligence Technology, Zhangjiang Lab, Shanghai, China. [8]Shanghai Key laboratory of Brain Function Restoration and Neural Regeneration, Shanghai, China. [9]These authors contributed equally: Yanming Zhu, Min Xu, Junfeng Lu, Jianhua Hu. ✉e-mail: wujinsong@huashan.org.cn; tanlh@sions.cn

comprehension[40]. fMRI studies found that cortical sites contributing to the syntactic analysis of Chinese phrases overlapped with cortical sites relevant to semantic analysis[23], and that nouns and verbs in Chinese activated a wide range of overlapping brain areas in distributed networks[41]. A recent fMRI study by Wu et al[42] showed a crucial role of both BA 44 and BA 45 in the left IFG in Chinese phrase structure building. They considered the involvement of BA 44 in syntactic computation to be language universal, whereas the role of BA 45 may be language specific and related to heavy reliance on contextual semantic information for Chinese processing. Thus, syntactic processing is less independent, and semantics and syntax are often not clearly demarcated in Chinese. Because of the inherent properties of Chinese syntax, it represents an important case for any attempt to examine the functional organization of syntactic processing, especially to determine whether the human brain implements syntactic structures independent of semantics.

Results

We recorded neural activity from ten native Mandarin-speaking participants (six right-handed females; 19–50 years of age) undergoing awake brain-mapping procedures as part of their brain tumour surgery. We recorded cortical activity using two 128-electrode grids that were located on the surface of the exposed cortex (Supplementary Fig. 1), while participants processed Chinese sentences and determined whether the presented written sentences were correct (Fig. 1a). Most participants responded fast and accurately during the task (Supplementary Fig. 2b). We focused on the electrodes in the left IFG (Methods). A classic violation paradigm was utilized to facilitate the comparison of our findings with previous studies with similar paradigms on alphabetic languages. We hypothesized that keywords that elicited violations would recruit additional neural resources to process corresponding linguistic aspects.

All the participants performed tasks in four conditions, including: (1) correct sentences (CORR), where the sentences were of normal subject–verb–object (SVO) structure; (2) syntactic violation of local phrase (SYN-P), where a degree adverb that was used to modify adjectives was inserted immediately before the object noun, which rejected the modification by the adverb; (3) violation of syntactic category (SYN-C), where the object noun was replaced by an adjective, which cannot be the direct object of the verb; and (4) semantic violation (SEM), where the object contradicted the selectional restrictions of the verb, which required an animate object (see Methods for more information). In all of the correct and violation conditions, the first-object nouns served as the keywords (Fig. 1a). Additionally, five participants performed a combined violation task (COM, five participants) that contained both syntactic and semantic violations (Supplementary Fig. 2c), and the other five participants performed a non-linguistic (NL) task as a non-language baseline (NL, five participants) in which they were presented with a series of geometric shapes and instructed to detect whether the shapes changed or not (Supplementary Fig. 2c). The NL task was used to test whether the enhanced activity elicited by violation manipulations was specific to linguistic processing or owing to a general violation processing.

We first used classification algorithms to examine the frequency component to best classify conditions in the linguistic task. Results showed that high-gamma (HG) components (>70 Hz) discriminated conditions with the highest accuracy (>80%, Fig. 1b and Supplementary Fig. 3a) and ERPs were more prominent in the HG band (70–150 Hz) compared with other frequency bands (Supplementary Fig. 3b–e). Most of the electrodes showing enhanced activities to linguistic stimuli were located in the IFG (Fig. 1c and Supplementary Fig. 3f). In contrast, in the NL task, the violation condition showed an enhanced activity mainly at the lower frequency (Supplementary Fig. 4), indicating that neural oscillations during linguistic and NL tasks may arise in
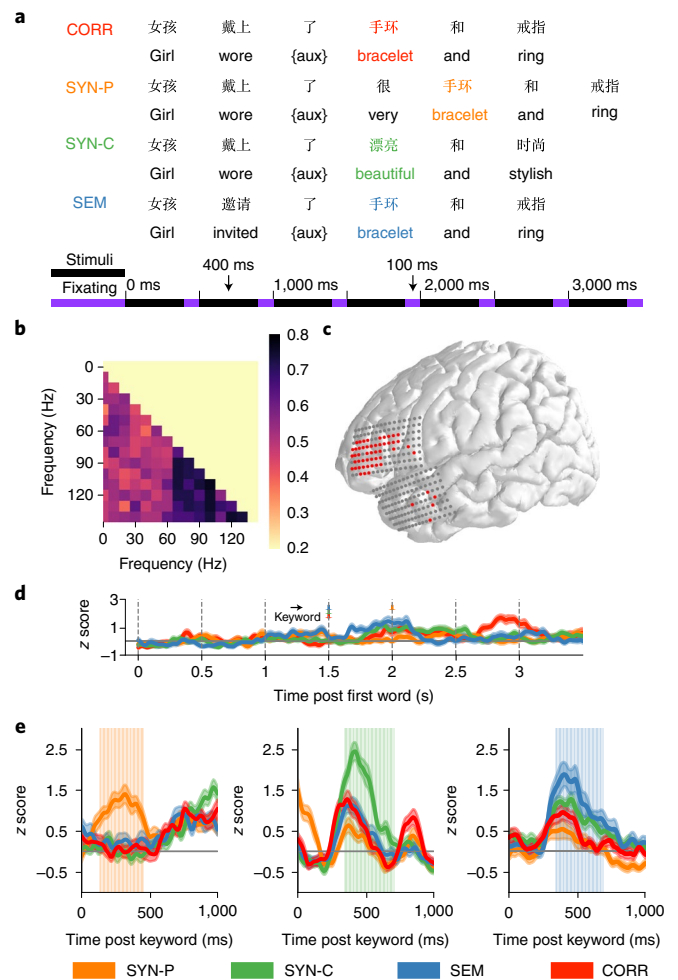
Fig. 1 | Study paradigm and different neural responsivity to semantic and syntactic violation tasks. a, Examples of stimuli in the sentence processing task. The words marked as their corresponding colour are the keywords for analyses unless otherwise specified. Correct sentences (CORR, red); syntactic violation of local phrase (SYN-P, orange); violation of syntactic category (SYN-C, green); semantic violation (SEM, blue); the black line indicates word stimuli presenting time (400 ms) and the purple line indicates fixation time (100 ms). **b**, Classification accuracy from an array of frequency bands using the support vector clustering, indicated that 70–150 Hz is the best frequency band to interpret the difference in processing each of the corresponding linguistic components. The x axis indicates the lower frequency boundary and the y axis indicates the upper-frequency boundary. **c**, MRI reconstruction of participant 3's brain with high-density grid electrodes (grey). Electrodes that responded to linguistic stimuli were labelled in red (Methods). **d**, Cortical activity for representative electrodes from the first presentation word to the last word of one participant; the coloured arrow indicates the onset of the keyword (mean ± s.e.m.). **e**, Cortical activity for representative electrodes after the keyword (mean ± s.e.m.). The shaded area corresponds to the discriminating period (P < 0.05, ANOVA, two tailed, Bonferroni correction for the number of electrodes).

different frequency bands. Hence, in the following analyses, we focused only on HG for electrodes at the IFG (70–150 Hz). In the linguistic task, the enhanced activity of violation conditions relative to CORR was only observed after the keywords, indicating that the responses were highly linked to the violation manipulations (Fig. 1d). Representative electrodes (shown in Fig. 1e) further verified that the manipulation of semantic or syntactic conditions
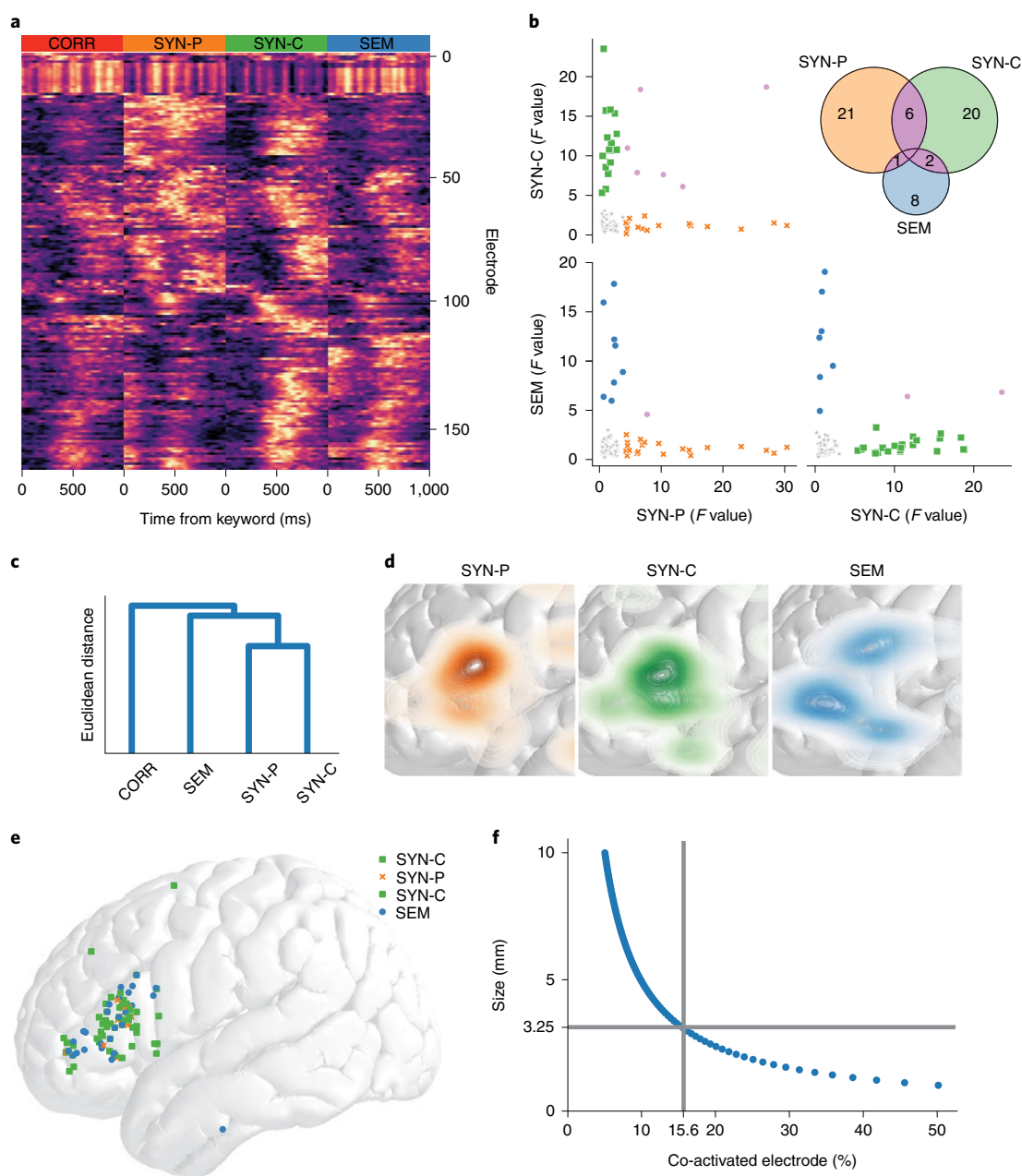
Fig. 2 | Spatial representation of syntax and semantics. a, Clustered time course from all responding electrodes. **b**, *F* value of responding electrodes to each violation condition and Venn diagram. The *F* value was from the comparison of respective violation sentences with the correct sentences for each responding electrode. **c**, Euclidean distance of the response to each linguistic condition; the *y* axis indicates the relative distance. **d**, KDE analysis for the centre of each linguistic feature processing. **e**, Permutation test for the epicentre of each violation condition. **f**, Simulation of the diameter of each functional circuit.

caused enhanced neural activities ($P < 0.05$ for one-way analysis of variance (ANOVA) between CORR and the relevant violation is shown as shaded area). The responses were consistent across trials (Supplementary Fig. 5).

We then examined whether there were electrodes specifically responding to syntactic or semantic violation conditions. We found that the responses of electrodes were dissimilar for different conditions across electrodes (Fig. 2a). To examine whether the electrodes responded to only one type or multiple types of violations, we defined a significant effect in each electrode if its response to a certain type of violation was reliably enhanced compared with the CORR condition for more than 50 ms ($P < 0.05$, ANOVA, two-tailed, Bonferroni correction for the number of electrodes, $n = 256$

for each participant); there were 58 electrodes satisfying this criterion and they were used for the following analyses. We found that most of the electrodes (49 of 58) strongly responded to only one type of violation (Fig. 2b, one-way ANOVA *F* statistic > 4). Only a few electrodes were co-activated by two violation types (9 of 58) and were mainly co-activated by SYN-P and SYN-C (as shown in purple in Fig. 2b). Additionally, we used half the trials to identify the linguistic-responding electrodes and used the remaining half for further analysis. We also quantified the length of time that the electrodes were responding differently to the violation conditions and to the correct condition. Both of the analyses based on amplitude and length of time yielded consistent patterns of results (Supplementary Fig. 6). This result was further supported by the degrees of

similarity across conditions as indexed with Euclidean distance, which showed that the similarity between SYN-P and SYN-C (Euclidean distance, 48.43) was greater than that between syntactic and semantic conditions (Fig. 2c, Euclidean distance, 62.17). Moreover, we found that, for the electrodes responding to the combined violation condition (COM), 78.3% of them also showed enhanced activity to the syntactic violation (SYN-P), but only 26.1% of them responded to the semantic violation (SEM), which may indicate a functional primacy of syntactic analysis (Supplementary Fig. 7a). In addition, the electrodes responding to linguistic stimuli did not respond to the NL violation, indicating that these electrodes' response was specific to linguistic processing (Supplementary Fig. 7b). These results showed that the neural responses to syntactic processing were spatially separated from semantic processing and NL processing at the single electrode level.

Subsequently, to examine whether there were spatial segregations for syntactic versus semantic processing on a larger scale, we applied a kernel-density estimation (KDE) analysis to characterize the spatial topographic organization and localize the activation centre for each condition (Fig. 2d and activation likelihood estimation in Supplementary Fig. 8a). Unlike the result at the electrode level, we failed to observe a tendency of spatial separation for the activation centre of syntactic and semantic conditions. Likewise, the epicentre of these responses failed to show separations using a permutation test of the clusters of electrodes (Fig. 2e). One possibility was that interindividual neuroanatomical variation of the IFG may lead to spatial overlap for different conditions when pooling over individuals. However, even at the individual level, we were unable to obtain a clear separation pattern (Supplementary Fig. 8b).

We quantified the scale at which semantic and syntactic processes were separated using a simulation method. We hypothesized that sections of IFG that had distinct coding for different linguistic components were tessellated. We simulated the percentage of electrodes that covered adjacent areas and then compared it with the percentage of electrodes that we observed of co-enhancement. The results showed that the diameter of functional circuits was no greater than ~3.25 mm (Fig. 2f)[43]. Overall, these results suggested that the electrodes specifically associated with syntactic and semantic processing were distributed independently at the electrode level.

Next, we hypothesized the spatiotemporal patterns elicited by the violation manipulations would be preserved when the correct sentences were processed. Using a prediction algorithm based on responses to CORR, our data showed the predicted electrode types with accuracies significantly higher than chance level (SYN-P 45.6%, SYP-C 73.0%, SEM 69.3%, and not-responding electrodes 38.4%; all $P < 0.0001$ relative to chance level 25%, Supplementary Fig. 9), suggesting that the electrodes specifically responding to syntactic or SEMs were also engaging in processing syntactic or semantic information when processing correct sentences.

We then examined the temporal properties of syntactic and semantic processing. The time courses of some example electrodes in Fig. 3a showed that there were differentiated temporal patterns for different types of violations. The accuracies for classifying different conditions peaked at about 400–700 ms after the keywords, which indicated they were most separable in this time frame (Supplementary Fig. 10a). We pooled all responding electrodes and found distinct response onsets and peaks for electrodes responding to different conditions (Fig. 3b,c). To quantify the temporal differences between different conditions, we estimated the latency differences based on ANOVA (Fig. 3d, $P < 0.001$, one-way ANOVA, two tailed, Bonferroni, corrected for ten participants. SEM onset to SYN-P onset, $P = 1.83 \times 10^{-5}$; SEM onset to SYN-C onset, $P = 1.93 \times 10^{-14}$; SYN-C onset to SYN-P onset, $P = 5.85 \times 10^{-30}$; SEM peak to SYN-P peak, $P = 3.26 \times 10^{-13}$; SEM peak to SYN-C peak, $P = 1.02 \times 10^{-5}$; SYN-C peak to SYN-P peak, $P = 0.93 \times 10^{-26}$). The results suggested that the SYN-P (onset, 113 ms and peak, 480 ms)

occurred earlier than SEM (122 ms and 524 ms) and SYN-C (283 ms and 579 ms) in terms of both onset and peak of the response, respectively. The onset and peak for SYN-P were earlier than for SYN-C. In SYN-P, the violation was detected immediately when encountering the adjective, but in SYN-C, the violation may be processed in a different way. In Chinese, disyllabic (or polysyllabic) adjectives are not directly attached to the head noun they modify. For example, if we add a noun to the position after the adjective, the modifier DE '的' should be added after the adjectives. Therefore, in SYN-C, the participants may detect the violation either when encountering the keyword (that is, the first objective) or when realizing that no DE '的' was coming after the adjective. This possibility may help explain the results that relatively later (and also greater variations of) onset and peak were observed for SYN-C than SYN-P.

There was also a discrepancy in terms of the length of the difference between respect violation and correct sentence (Supplementary Fig. 10b). Moreover, response latencies did not depend on the spatial location of the electrodes (Fig. 3e and Supplementary Fig. 10c,d).

Discussion

Together, the results demonstrated distinct spatiotemporal patterns of activity in the left IFG that were specifically associated with syntactic and semantic processing, indicating that this region was differentiated into distinct circuits that independently processed syntactic and semantic information in their corresponding time courses. Thus, these results offer strong evidence for the universality theory of syntactic processes[1,44–46].

Previous studies have argued for the non-independence of syntax in Chinese comprehension. The fast-changing neural activity and the adjacent presence of multiple functional groups explained why previous fMRI and scalp electrophysiology studies did not capture the fine-scale spatiotemporal patterns. The fine structure of activity may be obscured by the standard, local, average methods applied in previous neuroimaging research leading to a failure to consistently observe syntax specificity at the macroscopic regional level. In our study, we were able to record HG oscillations that are closely correlated with neuronal firing[47,48] and more suitable for local computations[49], providing greater specificity in cortical circuit mapping of syntactic and semantic processing. Our result is also in accordance with a previous study using intracranial electrophysiology[50], which identified spatiotemporally distinct patterns of activity for processing different linguistic components in IFG.

The differentiation of brain functions is important for establishing functional segregation as a principle of brain organization[51], and it entails computational advantages that enable efficient processing of information from different domains while minimizing interference[52]. Our findings revealed that syntactic and semantic processes in Chinese were implemented as a heterogeneous mix of modules at distributed circuits without clustering into distinct subregions in the left IFG. Yet, it remains possible that the neural level at which the two processes can be differentiated may be modulated by cross-linguistic variations in the degree to which syntax and semantics are separated. This explanation is consistent with some previous fMRI studies showing clear spatial separation of syntactic and semantic processing at the subregion level in morphologically rich languages such as German[53,54]. Our findings are essential to advance the understanding of the universality and specificity of neural mechanisms and neural decoding underlying human language[55–57]. An important goal for future research will be to characterize the interaction between different subcomponents and modules of language at both finer and larger brain scales to better understand the computational architecture of language processing.

In our study, we targeted the modularity theory of syntax and tested whether syntax and semantics operated independently during Chinese sentence processing by making a distinction between syntactic selection restriction and semantic selection restriction.
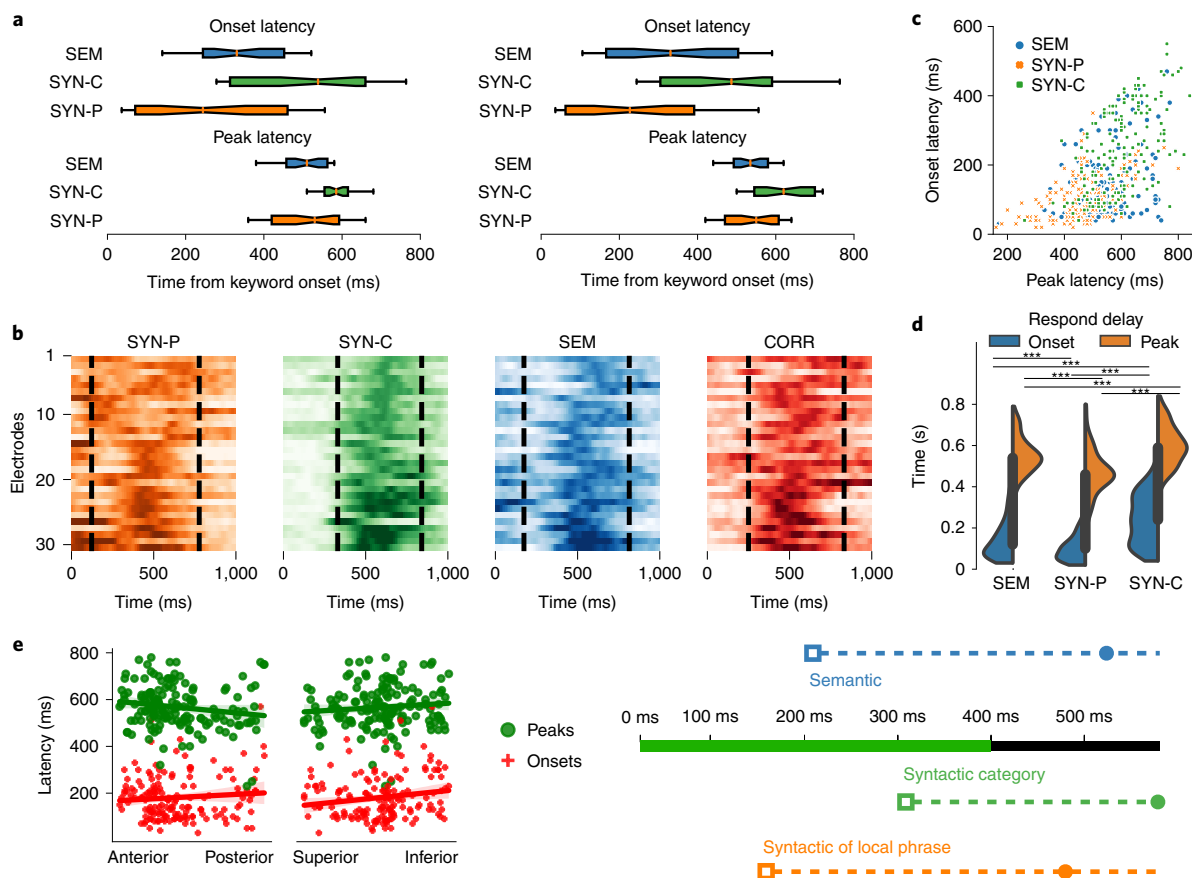
Fig. 3 | Temporal representation of syntax and semantics. a, Example electrodes showing temporal dissociations of different conditions (the box centre defined as the mean of the data; the box extends from the first quartile to the third quartile of the data, with a line at the median; the whiskers extend from 10% to 90% of ranked data). **b**, Time course of each condition with top 30 responding electrodes ranked by responding amplitude. Black-dashed lines indicate averaged onset and offset. **c**, Onset, and peak delay of all responding electrodes. **d**, Quantification of responding onset and peak (left) and comparison among SYN-P, SYN-C, and SEM. ***$P < 0.001$, one-way ANOVA, two tailed, Bonferroni corrected, $n = 106$, electrodes in pars opercularis, pars triangularis and precentral. **e**, Peak latency along anterior–posterior and superior–inferior axis. The x axis is the x or y coordinate of electrodes and the y values are their responding peaks and onset time (solid line, linear regression model for the location and latency; shaded colour area, 95% confidence interval of the linear regression model). **f**, Summary of the temporal dissociation. Filled circles denote response peak; hollow squares denote response onset.

There are alternative linguistic theoretical frameworks, some of which advocate an integrated view of syntax and semantics, such as construction grammar and usage-based grammar. A subscriber to theories such as these might question whether our experimental conditions were able to selectively tap syntactic as opposed to semantic processing, or even whether this is a useful distinction at all. For instance, the construction grammar approach[58] proposes a principle that "a construction is posited in the grammar if and only if something about its form, meaning, or use is not strictly predictable from other aspects of the grammar", although it emphasizes the importance of the requirements of the construction and the role that constructions play in the relationship between the form and meaning of simple sentences. However, we believe that in the cases involved in our discussion, no conflict arises between the requirements of the construction and those of the verb. Hence, even construction grammar would not attempt to account for these two restrictions in a way fundamentally different from ours, as there are no construction requirements involved in those cases under discussion.

We note that the present study has limitations. First, we used simple geometric shape judgement as a control task to exclude the possibility that the enhanced activity elicited by violation manipulations was due to a general violation processing, but we would need a broader range of control conditions, including linguistic violation control (for example, using a spelling violation task) and NL

violation control (for example, using music or arithmetic expressions), to give stronger evidence for the specificity of syntactic and semantic processing. Second, the keywords in SYN-C were not matched with other conditions in terms of syntactic categories (that is, the keywords in SYN-C were adjectives while in CORR/SEM/SYN-P were nouns). This factor may lead to differential spatiotemporal patterns between SYN-C and other conditions. However, it should be noted that the keywords in SYN-P were the same as those in SEM, but still, we found that more electrodes were co-activated by the two syntactic conditions (SYN-P and SYN-C) than those co-activated by SYN-P or SEM, and that the degree of similarity between SYN-P and SYN-C was greater than between syntactic and semantic conditions. The results suggest that distinct spatiotemporal activation patterns for syntactic and semantic conditions cannot be fully explained by the differences in the lexical or syntactic categories. Future studies are needed to understand how this confundity may influence critical effects.

Methods

Participants. This study included ten participants (age range, 19–50 years; four males, six females) undergoing awake language mapping as part of their brain tumour surgeries[59] at Huashan Hospital, Shanghai, China (Supplementary Table 1). Two 128-channel high-density ECoG grids were temporarily placed onto the left inferior/middle frontal gyrus and/or middle/superior temporal gyrus intraoperatively, to record cortical local field potential. Grid placement was

performed by an experienced neurosurgeon, and the location was determined based on clinical exposure and avoidance of the tumour. Because not all the participants were covered over the temporal cortex, and the location of the grids in the temporal cortex varied considerably across participants, our analyses focused on the electrodes in the IFG.

The study was approved by the Huashan Hospital Institutional Review Board of Fudan University (HIRB, KY2017–437), and the conducting of research complied with all relevant ethical regulations. Participants were asked to join this study only if there was clinical necessity to perform awake surgery for safe resection of tumour and protection of the eloquent area. Before surgery, the surgeon explained to participants that this task was for research purposes, that participation in the research was completely voluntary, that the research session would add 15–25 min to the length of their surgery and that they could stop the research session at any time. All participants consented voluntarily.

All participants were native speakers of Mandarin Chinese and were left dominant. They were cognitively healthy, as evaluated by the Mini-Mental State Examination, and had normal overall preoperative language functions using the Aphasia Battery of Chinese[60], which was the Chinese standardized adaptation of the Western Aphasia Battery. We only included those participants with tumours that did not obviously invade the pars opercularis and pars triangularis.

MRI acquisition. All preoperative brain images were obtained using a 3-T scanner (MAGNETOM Verio 3.0 T, Siemens AG) 1 day before surgery, and the imaging parameters were the same for all participants. The imaging protocols consisted of a three-dimensional T1-weighted high-resolution structural MRI (repetition time, 1.90 ms; echo time, 2.93 ms; matrix size, 256 × 215; slice thickness, 1 mm; field of view, 250 × 219 mm²) without contrast enhancement.

Cortical surface extraction and electrode visualization. Grids were localized by recording the three-dimensional positions of the corners of the grid using Medtronic neuronavigation system, Stealthlink (StealthStation Treon, Medtronic, Minneapolis, Minnesota, USA), and intraoperative photograph at the time of placement, then aligned to presurgical structural MRI (T1 weighted). The remaining electrodes were localized using interpolation from those points. To visualize electrodes on the cortical surface of a participant's brain we used FreeSurfer (v.1.0, February 2011, http://surfer.nmr.mgh.harvard.edu/) and img_pipe[61] to make pial surface reconstructions. The grid location is verified by two experienced neurosurgeons independently. To visualize electrodes across participants on a common Montreal Neurological Institute (MNI) brain, we performed non-linear surface registration using a spherical sulcal-based alignment in FreeSurfer[62], aligned to the MNI152 template[62]. While the geometry of the grid is not maintained, the non-linear alignment ensures that electrodes on a gyrus in the participant's native space will remain on the same gyrus in the atlas space.

The Chinese language and stimuli design. The Chinese language differs from the Indo–European languages (such as English) in many respects. Chinese is a morpho-syllabic system in which the characters map onto syllable units that are also usually morphemes. As a tonal language, every syllable in Chinese carries one of four basic tones, with different pitches of the voice conveying different meanings. Chinese is a non-inflected language that lacks morphological devices, and it has virtually no conjugation for verbs and no declension for nouns, which is in contrast to the rich inventory of grammatical morphology that marks syntactic features (such as a person, number, sex, case and tense) in Indo–European languages. With respect to syntactic categories, the distinction between noun and verb classes is transparent in Indo–European languages, but it is ambiguous in Chinese because of the lack of grammatical morphology that marks the syntactic category. Grammatical relations in Chinese are not generally manifested by morphological inflection but are cued by word order, function words and semantic content.

To facilitate the comparison between our results and those from Indo–European languages, the experimental conditions were designed to mirror the violations (that is, word category violation for syntactic violation and verb's selectional restriction violation for SEM) used by previous ERP studies of Indo–European languages such as German and French[63,64]. Different from previous studies of Indo–European languages, the word category of the critical word is not marked by grammatical inflections in our study due to the fact that Chinese generally lacks grammatical inflections. We took advantage of this property in Chinese to examine whether syntax constitutes an independent module in the human brain. In this study, the visual stimuli consisted of Chinese sentences of each condition (correct sentences (CORR), syntactic violation of local phrase (SYN-P), violation of syntactic category (SYN-C) and sentences with the SEM, and combined violation containing both SYN-P and SEM (COM)), and non-linguistic stimuli with or without shape-changing (NL and NL-VIO) displayed on a screen in front of the participants, with each word of the sentences or each geometric shape displayed sequentially in the centre of the screen. Each sentence was of SVO structure and the first-object nouns were served as the keywords. In CORR (for example, 女孩戴上了手环和戒指 (Girl wore bracelet and ring)), the keyword '手环 (bracelet)', as a noun, could be used as the object of the verb '戴 (wore)', thus satisfying the subcategorization requirement of the verb. In SYN-P (for example, 女孩戴上了很手环和戒指 (Girl wore very bracelet and ring)), the syntactic

violation occurred because a degree adverb '很 (very)' that was used to modify adjectives was inserted immediately before the object noun, which rejected the modification by the adverb. There were five different adverbs used in the SYN-P sentences. In SYN-C (for example, 女孩戴上了漂亮和时尚 (Girl wore beautiful and stylish)), syntactic violations occurred because the object noun '手环 (bracelet)' was replaced by an adjective '漂亮 (beautiful)', which cannot be the direct object of the verb. In SEM (for example, 女孩邀请了手环和戒指 (Girl invited bracelet and ring)), the sentences were well formed syntactically, but the object '手环 (bracelet)' contradicted the selectional restrictions of the verb '邀请 (invited)', which required an animate object. In COM, there were both syntactic (SYN-P) and SEMs (for example, 女孩邀请了很手环和戒指 (Girl invited very bracelet and ring)). We included two syntactic conditions to better match the stimuli across conditions. Both SYN-P and SYN-C involved a syntactic word category violation (that is, adjective instead of a noun), but in SYN-P, the violations occurred relative to the immediately preceding word, whereas, in SYN-C, the violation occurred relative to more distant preceding words (the verbs) in the sentences. The keywords in SYN-P were the same as those in CORR and SEM, and the keywords in SYN-C were presented in the same position as those in CORR and SEM. All the keywords were of two characters, and the word frequencies were matched between CORR (same in SYN-P and SEM, mean frequency = 31.88 per million, s.d. = 35.14) and SYN-C (mean frequency = 30.25 per million, s.d. = 73.58) ($t(62) = 0.11$, $P = 0.91$) (https://lingua.mtsu.edu/chinese-computing/). The participants were required to determine whether the sentences were correct. In the NL task, the participants were presented with a series of geometric shapes and instructed to detect whether the shapes changed. All the ten participants performed under CORR, SYN-P, SYN-C and SEM conditions. Five participants performed under COM and the other five performed under NL conditions.

All participants were trained to familiarize themselves with the study settings the day before the operation, as well as immediately before the experimental blocks. The sentences were displayed using custom-written MATLAB R2014a (Mathworks, https://www.mathworks.com) scripts. The stimuli were divided into four blocks and were presented randomly only once. Each trial started with an 800 ms fixation followed by a 500 ms blank screen, and then each word of the sentence (or geometric shape) was displayed for 400 ms, with a 100 ms interstimulus interval. There were six words per sentence in the CORR, SYN-C and SEM conditions and seven words in the SYN-P and COM conditions. The number of geometric shapes in the NL was matched to the number of words in the linguistic task. At the end of each trial, the participants were asked to decide whether the sentence was correct (or whether the geometric shapes changed) and they responded by clicking a button placed beneath the participant's index. The question remained on the screen until the participants responded or for a maximum of 3 s.

Neural data acquisition and preprocessing. We recorded ECoG signals with a multichannel amplifier (Tucker-Davis Technologies (TDT)) which was connected to a digital signal acquisition system (TDT), with a sampling rate of 3,052 Hz. The visual stimulus was also recorded via a photodiode from the output of the presentation screen and recorded in the TDT circuit, time-aligned with the ECoG signal. Data were online referenced in the amplifier and the reference electrode was placed onto the skull at the Central zero (Cz) point. No further re-referencing was applied to the data. Offline preprocessing of the data included the exclusion of bad channels, and exclusion of bad time intervals, concatenation of all experimental blocks, down-sampling to 400 Hz, notch-filtering of line noise at 50, 100 and 150 Hz, and common average reference (64 channels were connected to one bank). Bad channels were defined by visual inspection as channels with excessive noise. Bad time points were defined as time points with noise activity, which typically stemmed from movement artifacts, interictal-like spiking or non-physiological noise.

Data analysis. All analyses were conducted in MATLAB R2018 (Mathworks, https://www.mathworks.com) and Python (Python Software Foundation, Python Language Reference, v.3.7 or 2.7) using standard toolboxes and custom-written scripts, if not otherwise mentioned.

Frequency component extraction. To determine which frequency components were the most sensitive to distinguish the stimuli, we extracted the analytic amplitude of a band from 0 Hz to 150 Hz with 10 Hz intervals in the same manner. The power of each component was calculated as the first principal component of the signal in each electrode across each band-pass (the band is automatically assigned within script). The following frequency range decodings were based on the resulting timer series and using Scikit-learn library[65] for Python v.3.7. We used support vector machine (C=1.0, cache_size=200, class_weight=None, coef0=0.0, decision_function_shape='ovr', degree=3, gamma='auto', kernel='rbf', max_iter=−1, probability=False, random_state=None, shrinking=True, tol=0.001, verbose=False), logistic regression (C=1.0, class_weight=None, dual=False, fit_intercept=True, intercept_scaling=1, max_iter=100, multi_class='auto', n_jobs=None, penalty='l2', random_state=None, solver='newton-cg', tol=0.0001, verbose=0, warm_start=False) and k-nearest neighbour (algorithm='auto', leaf_size=30, metric='minkowski', metric_params=None, n_jobs=None, n_neighbors=5, p=2, weights='uniform') to classify different conditions, that

is, correct sentences, sentences with syntactic violation, sentences with semantic violation and resting state.

We extracted the analytic amplitude in the HG frequency range (70–150 Hz, High gamma activity (HGA)) using eight band-pass with the Hilbert transform. The HGA power was calculated as the first principal component of the signal in each electrode across all eight HG bands, using principal component analysis. Finally, the HGA was down-sampled to 100 Hz and z scored relative to the mean and standard deviation of the data within each experimental block.

Electrode selection. Analyses included electrodes located in all covered cortices on the pars opercularis and pars triangularis (the notation is in accordance to FreeSurfer segregation) that showed robust evoked responses to the stimuli, defined as electrodes by the difference of the cortical response between resting state versus linguistic/NL stimuli explained with a significant amount of variance ($P < 0.01$, Python scipy library one-way ANOVA function f_oneway). As the neural signal was z scored before further analysis, the neural signal may be considered to have normality and equal variances for further analysis.

We could observe enhanced activities after the keywords (Fig. 1d); however, the electrodes should have enhanced activities to all words if they were deemed as 'language-responsive/sensitive' electrodes. The reason it was hard to observe amplitude peaks after non-keyword words was because we z scored the signal across the block; although there were peaks in non-keyword words, z scoring would amplify the strongest peak and dwarf lower peaks. The power spectrum analysis, on the other hand, using log-scale representation, showed enhanced activities to all meaningful words (except for auxiliary words/non-meaning words).

Here, we defined the SYN-P, SYN-C or SEM electrode as an electrode that had its averaged amplitude reliably higher than the amplitude under CORR (f_oneway with Bonferroni correction for more than 50 ms and >0.55 z score in amplitude). Here, we compared two groups at a given time; we compared the correct sentences with one type of violation condition alone, then with the second condition, then the third one. The time-course similarities (Euclidean distance) among each linguistic stimuli were performed using the Python scipy library hierarchical clustering function.

ERP amplitude. To compare evoked responses among each experimental condition (CORR, SYN-P, SYN-C and SEM). Mean neural responses to individual keywords for each electrode were calculated for the selected electrodes. We aligned the cortical activity to the onset of the keyword as the T0 for presentation. The discriminating period is defined as one-way ANOVA of response to CORR sentences versus SYN-P, SYN-C or SEM sentences, $P < 0.05$, ANOVA, two tailed, Bonferroni correction for the number of electrodes, $n = 256$ for each participant. The onset, peak and offset were defined as 10%, 50% and 90% of the ERP integer. The fractional area latency measure would then be defined as the time point before which a certain percentage of the total ERP area was observed. Here, we did not utilize arguments of the maxima, simply because the local field potential is a sinusoidal wave with many fluctuations or noise, the local arguments of the maxima are largely influenced by local fluctuations or noise, thus using a 50% local field potential integer is a better alternative to avoid fluctuations or noise, and this method is indifferent to the amplitude difference between electrodes or trials.

Spatial organization. To summarize the electrode location from multiple participants and avoid bias, we utilized the KDE (bandwidth = 20) and activation likelihood estimation (cluster-level family-wise error with 1,000 permutations of $P < 0.01$, GingerALE v.2.3.6, http://www.brainmap.org) method to cluster the selected electrode locations with on the MNI152 template, and the results were visualized two dimensionally (overlap onto two-dimensional brain) or three dimesionally (BrainNet Viewer, http://www.nitrc.org/projects/bnv/). This technique transforms the extracted electrodes, and the difference between SYN-P, SYN-C and SEM, into Gaussian probability distributions surrounding the coordinates. The estimation of the width of these Gaussian probability distributions is adapted for each condition using the relative density. Non-parametric permutation tests were performed to determine the spatial segregation among SYN-P, SYN-C and SEM.

Functional circuit size estimation. We hypothesize that the entire IFG is tessellated with multiple functional circuits that process different functions independently. We assume the size of a functional circuit that processes different linguistic features should be similar, and the distribution of electrodes was randomized. If an electrode (radius of 0.5 mm) covered both adjacent functional circuits, then this electrode would record the activity of both areas. Given the percentage of electrodes that responded to two violation conditions, we could estimate the size of each functional circuit.

$$p\,(\text{co-activation}) = p\,(\text{distant (electrode centre to boundary)} \leq 0.5\ \text{mm})$$

$$= \frac{1 - A(\text{triangle with diameter of } r - 0.5\ \text{mm})}{A(\text{triangle with diameter of } r)} = \frac{r - 0.5\ \text{mm}}{r}$$

where p is the probability, A is the area and r is the diameter.

Predicting different types of electrodes using brain responses in CORR. When processing correct sentences, the cortical areas responsible for semantics or syntactic should still process the corresponding aspects. We hypothesized that even during correct stimuli, the electrodes should preserve their spatial–temporal prosperity like when they are processing incorrect stimuli. We labelled electrodes, then trained models using extracted information only from correct sentences (onset, offset, peak, area and amplitude at T0) to predict the electrode types (SYN-P, SYN-C, SEM or non-responding electrodes).

Reporting summary. Further information on research design is available in the Nature Research Reporting Summary linked to this article.

Data availability
Source data are provided with this paper. The data set generated during the current study will be made available from the authors upon reasonable request.

Code availability
The completely developed code that operates on the full data set will be made available from the authors upon reasonable request.

References

1. Hauser, M. D., Chomsky, N. & Fitch, W. T. The faculty of language: what is it, who has it, and how did it evolve? *Science* **298**, 1569–1579 (2002).
2. Chomsky, N. *Rules and Representations* (Columbia Univ. Press, 1980).
3. Fodor, J. A. *Modularity of Mind* (MIT Press, 1983).
4. Pinker, S. Rules of language. *Science* **253**, 530–535 (1991).
5. Dapretto, M. & Bookheimer, S. Y. Form and content: dissociating syntax and semantics in sentence comprehension. *Neuron* **24**, 427–432 (1999).
6. Friederici, A. D., Chomsky, N., Berwick, R. C. Moro, A. & Bolhuis, J. J. Language, mind and brain. *Nat. Hum. Behav.* **1**, 713–722 (2017).
7. Pylkkänen, L. The neural basis of combinatory syntax and semantics. *Science* **366**, 62–66 (2019).
8. Hagoort, P. The core and beyond in the language-ready brain. *Neurosci. Biobehav. Rev.* **81**, 194–204 (2017).
9. Pallier, C., Devauchelle, A. & Dehaene, S. Cortical representation of the constituent structure of sentences. *Proc. Natl Acad. Sci. USA* **108**, 2522–2527 (2011).
10. Grodzinsky, Y. The neurology of syntax: language use without Broca's area. *Behav. Brain Sci.* **23**, 1–21 (2000).
11. Tyler, L. K. et al. Left inferior frontal cortex and syntax: function, structure and behaviour in patients with left hemisphere damage. *Brain* **134**, 415–431 (2011).
12. Dronkers, N. F. A new brain region for coordinating speech articulation. *Nature* **384**, 159–161 (1996).
13. Embick, D., Marantz, A., Miyashita, Y. Oneil, W. & Sakai, K. L. A syntactic specialization for Broca's area. *Proc. Natl Acad. Sci. USA* **97**, 6150–6154 (2000).
14. Glaser, Y. G., Martin, R. C., Van Dyke, J. A., Hamilton, A. C. & Tan, Y. Neural basis of semantic and syntactic interference in sentence comprehension. *Brain Lang.* **126**, 314–326 (2013).
15. Hagoort, P. & Indefrey, P. The neurobiology of language beyond single words. *Annu. Rev. Neurosci.* **37**, 347–362 (2014).
16. Prat, C. S. & Just, M. A. Exploring the neural dynamics underpinning individual differences in sentence comprehension. *Cereb. Cortex* **21**, 1747–1760 (2011).
17. Hashimoto, R. & Sakai, K. L. Specialization in the left prefrontal cortex for sentence comprehension. *Neuron* **35**, 589–597 (2002).
18. Osterhout, L. & Holcomb, P. J. Event-related brain potentials elicited by syntactic anomaly. *J. Mem. Lang.* **31**, 785–806 (1992).
19. Friederici, A. D. The brain basis of language processing: from structure to function. *Physiol. Rev.* **91**, 1357–1392 (2011).
20. Kutas, M. & Federmeier, K. D. Thirty years and counting: finding meaning in the N400 component of the event-related brain potential (ERP). *Annu. Rev. Psychol.* **62**, 621–647 (2011).
21. Blank, I., Balewski, Z., Mahowald, K. & Fedorenko, E. Syntactic processing is distributed across the language system. *Neuroimage* **127**, 307–323 (2016).
22. Rogalsky, C. & Hickok, G. Selective attention to semantic and syntactic features modulates sentence processing networks in anterior temporal cortex. *Cereb. Cortex* **19**, 786–796 (2009).
23. Luke, K., Liu, H., Wai, Y., Wan, Y. & Tan, L. Functional anatomy of syntactic and semantic processing in language comprehension. *Hum. Brain Mapp.* **16**, 133–145 (2002).
24. Bautista, A. & Wilson, S. M. Neural responses to grammatically and lexically degraded speech. *Lang., Cognition Neurosci.* **31**, 567–574 (2016).
25. Fedorenko, E. & Varley, R. Language and thought are not the same thing: evidence from neuroimaging and neurological patients. *Ann. N. Y. Acad. Sci.* **1369**, 132–153 (2016).

26. Heim, S., Eickhoff, S. B. & Amunts, K. Specialisation in Broca's region for semantic, phonological, and syntactic fluency? *Neuroimage* **40**, 1362–1368 (2008).

27. Rodd, J. M., Vitello, S., Woollams, A. M. & Adank, P. Localising semantic and syntactic processing in spoken and written language comprehension: an activation likelihood estimation meta-analysis. *Brain Lang.* **141**, 89–102 (2015).

28. Dick, F. et al. Language deficits, localization, and grammar: evidence for a distributive model of language breakdown in aphasic patients and neurologically intact individuals. *Psychol. Rev.* **108**, 759–788 (2001).

29. Kaan, E. & Swaab, T. Y. The brain circuitry of syntactic comprehension. *Trends Cogn. Sci.* **6**, 350–356 (2002).

30. Fedorenko, E., Nietocastanon, A. & Kanwisher, N. Lexical and syntactic representations in the brain: an fMRI investigation with multi-voxel pattern analyses. *Neuropsychologia* **50**, 499–513 (2012).

31. Mesulam, M. M. et al. Primary progressive aphasia and the evolving neurology of the language network. *Nat. Rev. Neurol.* **10**, 554–569 (2014).

32. Wilson, S. M., Galantucci, S., Tartaglia, M. C. & Gornotempini, M. L. The neural basis of syntactic deficits in primary progressive aphasia. *Brain Lang.* **122**, 190–198 (2012).

33. Anumanchipalli, G. K., Chartier, J. & Chang, E. F. Speech synthesis from neural decoding of spoken sentences. *Nature* **568**, 493–498 (2019).

34. Li, C. & Thompson, S. *Mandarin Chinese: A Functional Reference Grammar* (Univ. of California Press, 1989).

35. Wang, W. S. Y. The Chinese language. *Sci. Am.* **228**, 50–62 (1973).

36. Li, P., Shu, H. & Liu, Y. in *The Handbook of Chinese Linguistics* (eds Huang, C.-T. J. et al.) (John Wiley & Sons, 2014).

37. Zhang, Y., Yu, J. & Boland, J. E. Semantics does not need a processing license from syntax in reading Chinese. *J. Exp. Psychol.: Learning Mem. Cognition* **36**, 765–781 (2010).

38. Scott, B. *Translation, Brains and the Computer. Machine Translation: Technologies and Applications* (Springer, 2018).

39. Liu, Y., Li, P., Shu, H., Zhang, Q. & Chen, L. Structure and meaning in Chinese: an ERP study of idioms. *J. Neurolinguist.* **23**, 615–630 (2010).

40. Ye, Z., Luo, Y., Friederici, A. D. & Zhou, X. Semantic and syntactic processing in Chinese sentence comprehension: evidence from event-related potentials. *Brain Res.* **1071**, 186–196 (2006).

41. Li, P., Jin, Z. & Tan, L. H. Neural representations of nouns and verbs in Chinese: an fMRI study. *Neuroimage* **21**, 1533–1541 (2004).

42. Wu, C., Zaccarella, E. & Friederici, A. D. Universal neural basis of structure building evidenced by network modulations emerging from Broca's area: the case of Chinese. *Hum. Brain Mapp.* **40**, 1705–1717 (2019).

43. Leise, E. M. Modular construction of nervous systems: a basic principle of design for invertebrates and vertebrates. *Brain Res. Rev.* **15**, 1–23 (1990).

44. Chomsky, N. *Language and Mind* 3rd edn (Cambridge Univ. Press, 2006).

45. Frazier, L. & Fodor, J. D. The sausage machine: a new two-stage parsing model. *Cognition* **6**, 291–325 (1978).

46. Friederici, A. D. Towards a neural basis of auditory sentence processing. *Trends Cogn. Sci.* **6**, 78–84 (2002).

47. Mukamel, R. et al. Coupling between neuronal firing, field potentials, and fMRI in human auditory cortex. *Science* **309**, 951–954 (2005).

48. Nir, Y. et al. Coupling between neuronal firing rate, gamma LFP, and BOLD fMRI is related to interneuronal correlations. *Curr. Biol.* **17**, 1275–1285 (2007).

49. Gregoriou, G. G., Gotts, S. J., Zhou, H. & Desimone, R. High-frequency, long-range coupling between prefrontal and visual cortex during attention. *Science* **324**, 1207–1210 (2009).

50. Sahin, N. T., Pinker, S., Cash, S. S., Schomer, D. L. & Halgren, E. Sequential processing of lexical, grammatical, and phonological information within Broca's area. *Science* **326**, 445–449 (2009).

51. Friston, K. J. & Price, C. J. Modules and brain mapping. *Cogn. Neuropsychol.* **28**, 241–250 (2011).

52. Kanwisher, N. Functional specificity in the human brain: a window into the functional architecture of the mind. *Proc. Natl Acad. Sci. USA* **107**, 11163–11170 (2010).

53. Goucha, T. & Friederici, A. D. The language skeleton after dissecting meaning: a functional segregation within Broca's area. *Neuroimage* **114**, 294–302 (2015).

54. Zaccarella, E. Meyer, L., Makuuchi, M. & Friederici, A. D. Building by syntax: the neural basis of minimal linguistic structures. *Cereb. Cortex* **27**, 411–421 (2015).

55. Siok, W. T., Perfetti, C. A., Jin, Z. & Tan, L. H. Biological abnormality of impaired reading is constrained by culture. *Nature* **431**, 71–76 (2004).

56. Perfetti, C. A., Cao, F. & Booth, J. Specialization and universals in the development of reading skill: how Chinese research informs a universal science of reading. *Sci. Stud. Read.* **17**, 5–21 (2013).

57. Nakamura, K. et al. Universal brain systems for recognizing word shapes and handwriting gestures during reading. *Proc. Natl Acad. Sci. USA* **109**, 20762–20767 (2012).

58. Goldberg, A. E. *A Construction Grammar Approach to Argument Structure* (Univ. of Chicago Press, 1995).

59. Lu, J. et al. Awake language mapping and 3-Tesla intraoperative MRI-guided volumetric resection for gliomas in language areas. *J. Clin. Neurosci.* **20**, 1280–1287 (2013).

60. Wu, J. et al. Direct evidence from intraoperative electrocortical stimulation indicates shared and distinct speech production center between Chinese and English languages. *Hum. Brain Mapp.* **36**, 4972–4985 (2015).

61. Hamilton, L. S., Chang, D. L., Lee, M. B. & Chang, E. F. Semi-automated anatomical labeling and inter-subject warping of high-density intracranial recording electrodes in electrocorticography. *Front. Neuroinform.* **11**, 62 (2017).

62. VS Fonov, A. E., McKinstry, R. C., Almli, C. R. & Collins, D. L. Unbiased nonlinear average age-appropriate brain templates from birth to adulthood. *NeuroImage* **47**, S102 (2009).

63. Friederici, A. D. & Meyer, M. The brain knows the difference: Two types of grammatical violations. *Brain Res.* **1000**, 72–77 (2004).

64. Hahne, A. & Friederici, A. D. Differential task effects on semantic and syntactic processes as revealed by ERPs. *Cognitive Brain Res.* **13**, 339–356 (2002).

65. Pedregosa, F. et al. Scikit-learn: machine learning in Python. *J. Mach. Learn. Res.* **12**, 2825–2830 (2011).

Author contributions

L.H.T. and J.W. conceived and supervised the project. J.L., M.X., Y. Zhu, V.P.Y.K., Y. Zhou, D.Y., B.W. and J.Z. collected the data. J.H., L.H.T., M.X., Y. Zhu, J.L. and J.W. designed the experiment. Y. Zhu, J.L. and M.X. analysed the data. Y. Zhu, J.L., M.X., J.H., J.W. and L.H.T. interpreted the data. Y. Zhu, M.X., J.L., J.H., J.W. and L.H.T. wrote the manuscript.

Competing interests

The authors declare no competing interests.

Additional information

Supplementary information The online version contains supplementary material available at https://doi.org/10.1038/s41562-022-01334-6.

Correspondence and requests for materials should be addressed to Jinsong Wu or Li Hai Tan.

Peer review information *Nature Human Behaviour* thanks Heidi Harley and the other, anonymous, reviewer(s) for their contribution to the peer review of this work. Peer reviewer reports are available.

Reprints and permissions information is available at www.nature.com/reprints.

Publisher's note Springer Nature remains neutral with regard to jurisdictional claims in published maps and institutional affiliations.

nature research

Corresponding author(s): Li Hai Tan, Jinsong Wu

Last updated by author(s): Nov 22, 2021

Reporting Summary

Nature Research wishes to improve the reproducibility of the work that we publish. This form provides structure for consistency and transparency in reporting. For further information on Nature Research policies, see our Editorial Policies and the Editorial Policy Checklist.

Statistics

For all statistical analyses, confirm that the following items are present in the figure legend, table legend, main text, or Methods section.

n/a	Confirmed	
☐	☒	The exact sample size (*n*) for each experimental group/condition, given as a discrete number and unit of measurement
☐	☒	A statement on whether measurements were taken from distinct samples or whether the same sample was measured repeatedly
☐	☒	The statistical test(s) used AND whether they are one- or two-sided *Only common tests should be described solely by name; describe more complex techniques in the Methods section.*
☒	☐	A description of all covariates tested
☐	☒	A description of any assumptions or corrections, such as tests of normality and adjustment for multiple comparisons
☐	☒	A full description of the statistical parameters including central tendency (e.g. means) or other basic estimates (e.g. regression coefficient) AND variation (e.g. standard deviation) or associated estimates of uncertainty (e.g. confidence intervals)
☐	☒	For null hypothesis testing, the test statistic (e.g. *F*, *t*, *r*) with confidence intervals, effect sizes, degrees of freedom and *P* value noted *Give P values as exact values whenever suitable.*
☒	☐	For Bayesian analysis, information on the choice of priors and Markov chain Monte Carlo settings
☐	☒	For hierarchical and complex designs, identification of the appropriate level for tests and full reporting of outcomes
☒	☐	Estimates of effect sizes (e.g. Cohen's *d*, Pearson's *r*), indicating how they were calculated

Our web collection on statistics for biologists contains articles on many of the points above.

Software and code

Policy information about availability of computer code

Data collection	Synapse Suite (Tucker-Davis Technologies, Alachua, FL, USA) Version 91
Data analysis	MATLAB R2018a (Mathworks, https://www.mathworks.com), and Python (Python Software Foundation. Python Language Reference, version 3.7 or 2.7), FreeSurfer Version 2.0 and custom code.

For manuscripts utilizing custom algorithms or software that are central to the research but not yet described in published literature, software must be made available to editors and reviewers. We strongly encourage code deposition in a community repository (e.g. GitHub). See the Nature Research guidelines for submitting code & software for further information.

Data

Policy information about availability of data

All manuscripts must include a data availability statement. This statement should provide the following information, where applicable:
- Accession codes, unique identifiers, or web links for publicly available datasets
- A list of figures that have associated raw data
- A description of any restrictions on data availability

The data set generated during the current study will be made available from the authors upon reasonable request. Source data are provided with this paper.

Field-specific reporting

Please select the one below that is the best fit for your research. If you are not sure, read the appropriate sections before making your selection.

☐ Life sciences   ☒ Behavioural & social sciences   ☐ Ecological, evolutionary & environmental sciences

For a reference copy of the document with all sections, see nature.com/documents/nr-reporting-summary-flat.pdf

Behavioural & social sciences study design

All studies must disclose on these points even when the disclosure is negative.

Study description	This is a quantitative basic research involves human subjects.
Research sample	Patients with glioma near eloquent area at Huashan Hospital.
Sampling strategy	No need for sampling.
Data collection	We recorded ECoG signals with a multichannel amplifier (Tucker-Davis Technologies, TDT, Alachua, FL, USA), which was connected to a digital signal acquisition system (TDT), with a sampling rate of 3052 Hz. The visual stimulus was also recorded via a photodiode from the output of the presentation screen and recorded in the TDT circuit time-aligned with the ECoG signal. Data were online referenced in the amplifier, the reference electrode was placed onto the skull at Cz point. No further re-referencing was applied to the data.
Timing	Mar.2, 2018 to Nov. 27, 2019
Data exclusions	Exclusion of bad channels, and exclusion of bad time intervals. Bad channels were defined by visual inspection as channels with excessive noise. Bad time points were defined as time points with noise activity, which typically stemmed from movement artifacts, interictal-like spiking, or non-physiological noise.
Non-participation	No participant dropped out.
Randomization	No need for randomization.

Reporting for specific materials, systems and methods

We require information from authors about some types of materials, experimental systems and methods used in many studies. Here, indicate whether each material, system or method listed is relevant to your study. If you are not sure if a list item applies to your research, read the appropriate section before selecting a response.

Materials & experimental systems

n/a	Involved in the study
☒	☐ Antibodies
☒	☐ Eukaryotic cell lines
☒	☐ Palaeontology and archaeology
☒	☐ Animals and other organisms
☐	☒ Human research participants
☒	☐ Clinical data
☒	☐ Dual use research of concern

Methods

n/a	Involved in the study
☒	☐ ChIP-seq
☒	☐ Flow cytometry
☐	☒ MRI-based neuroimaging

Human research participants

Policy information about studies involving human research participants

Population characteristics	This study included ten participants (age range: 19-50 years; 4 males, 6 females) undergoing awake language mapping as part of their brain tumor surgeries at Huashan Hospital, Shanghai, China.
Recruitment	Participants were asked to participate in this study only if they needed awake surgery with direct cortical stimulation as part of their language mapping, meaning this was essential for safe resection of their tumor and protection of eloquent area.
Ethics oversight	Huashan Hospital Institutional Review Board of Fudan University (HIRB)

Note that full information on the approval of the study protocol must also be provided in the manuscript.

Magnetic resonance imaging

Experimental design

Design type	Structural T1-weighted
Design specifications	n/a
Behavioral performance measures	n/a

Acquisition

Imaging type(s)	Structural
Field strength	3Tesla
Sequence & imaging parameters	repetition time, 1.90 ms; echo time, 2.93 ms; matrix size, 256×215; slice thickness, 1 mm; field of view, 250×219 mm2
Area of acquisition	Whole brain

Diffusion MRI ☐ Used ☒ Not used

Preprocessing

Preprocessing software	FreeSurfer
Normalization	A combination of volumetric and surface warping (Postelnicu et al., 2009)
Normalization template	cvs_avg35_inMNI152
Noise and artifact removal	None
Volume censoring	None

Statistical modeling & inference

Model type and settings	n/a
Effect(s) tested	n/a

Specify type of analysis: ☒ Whole brain ☐ ROI-based ☐ Both

Statistic type for inference (See Eklund et al. 2016)	n/a
Correction	n/a

Models & analysis

n/a	Involved in the study
☒	☐ Functional and/or effective connectivity
☒	☐ Graph analysis
☒	☐ Multivariate modeling or predictive analysis